LAWRENCE
LIVERMORE
NATIONAL
LABORATORY

LLNL-JRNL-410883

The Autoignition of iso-Cetane: Shock Tube Experiments and Kinetic Modeling

M. A. Oehlschlaeger, J. Steinberg, C. K. Westbrook, W. J. Pitz

February 27, 2009

Combustion and Flame

Disclaimer

Submitted to
Combustion and Flame
2/24/09

The Autoignition of iso-Cetane: Shock Tube Experiments and Kinetic Modeling

Matthew A. Oehlschlaeger, Justin Steinberg,
Department of Mechanical, Aerospace, and Nuclear Engineering,
Rensselaer Polytechnic Institute, Troy, New York, U.S.A.

Charles K. Westbrook, and William J. Pitz
Lawrence Livermore National Laboratory, Livermore, California, U.S.A.

Corresponding author:
Matthew Oehlschlaeger
110 8th St
JEC 2049
Troy, NY 12180
518-276-8115 (office tel)
oehlsm@rpi.edu

Abstract

Iso-cetane (2,2,4,4,6,8,8-heptamethylnonane, $C_{16}H_{34}$) is a highly branched alkane reference compound for determining cetane ratings. It is also a candidate branched alkane representative in surrogate mixtures for diesel and jet fuels. Here new experiments and kinetic modeling results are presented for the autoignition of iso-cetane at elevated temperatures and pressures relevant to combustion in internal combustion engines. Ignition delay time measurements were made in reflected shock experiments in a heated shock tube for $\Phi = 0.5$ and 1.0 iso-cetane/air mixtures at temperatures ranging from 953 to 1347 K and pressures from 8 to 47 atm. Ignition delay times were measured using electronically excited OH emission, monitored through the shock tube end wall, and piezoelectric pressure transducer measurements, made at side wall locations. A new kinetic mechanism for the description of the oxidation of iso-cetane is presented that is developed based on a previous mechanism for iso-octane. Computed results from the mechanism are found in good agreement with the experimental measurements. To our knowledge, the ignition time measurements and detailed kinetic mechanism for iso-cetane presented here are the first of their kind.

Keywords: shock tube, ignition, iso-cetane, 2,2,4,4,6,8,8 heptamethylnonane, kinetic modeling, mechanism

1. Introduction

Liquid transportation fuels are typically complex distillate mixtures comprised of hundreds to thousands of individual hydrocarbon compounds. Due to the large number of compounds found in these fuels, often simplified surrogate mixtures are formulated to mimic the chemical and physical properties of the fuel of interest, partly for the purposes of developing manageable kinetic mechanisms for combustion simulations and allowing controlled experiments for comparison to and validation of simulations. Surrogate compounds are often selected because they are representative of the compounds (e.g., similar structure, molecular weight, boiling point) found in the distillate fuel within each hydrocarbon classification (n-alkane, iso-alkane, cyclo-alkane, alkene, aromatic, etc.).

2,2,4,4,6,8,8-heptamethylnonane (iso-cetane, i-$C_{16}H_{34}$), a reference compound for the cetane number (CN) rating, is an important representative branched alkane and surrogate component candidate for diesel fuels [1], which typically contain alkane compounds in the C_{10}-C_{24} range [2]. Additionally, iso-cetane has applicability as a component for surrogate mixtures for jet fuels (Jet-A, JP-8) [3-4], which contain large quantities of alkanes (~30% normal and ~30% branched) in the C_9-C_{16} range [5].

The cetane number for diesel fuels is defined by matching the measured ignition delay time of a specific fuel spray, injected into a Cooperative Fuel Research (CRF) or in an Ignition Quality Tester (IQT) at specified conditions, to that of a binary mixture of the less ignitable branched iso-cetane (CN = 15) and the more easily ignitable straight-chain n-cetane (n-hexadecane, CN = 100). The CN can also be defined using mixtures of n-cetane and 1-methylnaphthalene (CN = 0). As a reference compound for cetane rating, iso-cetane is an excellent candidate as a branched alkane representative in diesel and jet

fuel surrogate mixtures and has been used in JP-8 surrogate mixtures by Agosta et al. [4] and been recommended by Farrell et al. [1] as a component in diesel surrogate mixtures. Farrell et al. suggest blends of n-cetane (n-hexadecane), iso-cetane, n-decylbenzene, and 1-methylnaphthane for surrogate diesel mixtures.

Despite its importance as a cetane rating reference compound and its potential utility in surrogate mixtures, there has been very little experimental and kinetic modeling effort dedicated to iso-cetane. This is in stark contrast to the branched alkane reference compound for research octane number (RON), iso-octane (2,2,4-trimethylpentane, RON = 100), for which there is a plethora of literature describing experimental and kinetic modeling studies (examples include [6-13]). Additionally, there have been noteworthy kinetics investigations for other moderate-sized branched alkanes including, for example, a series of experimental and modeling studies on the influence of branching structure on the high- and low-temperature ignition of the nine heptane isomers [14-17].

The lack of previous experimental and kinetic modeling studies for iso-cetane is primarily due to its large size, making kinetic oxidation mechanisms very large in terms of number of species and reactions and gas-phase experiments difficult due to the low vapor pressure of iso-cetane. The only previous experimental efforts related to iso-cetane, to our knowledge, are the flow reactor measurements of Agosta et al. [4] and Lenhert et al. [18] who measured low-temperature (600-800 K) reactivity, via CO production, and product speciation in a pressurized (8 atm) flow reactor for a lean dilute iso-cetane/O_2/N_2 mixture and a lean dilute blend of 60% iso-cetane and 40% n-dodecane in O_2 and N_2. Agosta et al. [4] also developed an iso-cetane kinetic scheme based on lumped reactions for simulation of and comparison to their flow reactor measurements of CO production.

Due to the importance of iso-cetane as a diesel reference compound and as a surrogate component candidate and the lack of previous kinetic study for this important branched alkane, here we present, to our knowledge, the first shock tube ignition delay time measurements for iso-cetane/air mixtures and a newly developed detailed iso-cetane kinetic oxidation mechanism. Ignition delay times were measured in an externally heated shock tube, enabling sufficient iso-cetane vapor pressure for the investigation of the homogenous gas-phase ignition of Φ = 0.5 and 1.0 iso-cetane/air mixtures at elevated pressures (8-47 atm) relevant to practical combustion environments (e.g., IC engines and gas turbines). Additionally, a detailed iso-cetane oxidation mechanism has been formulated, containing both low- and high-temperature chemistry, using reaction rate coefficient rules previously developed for iso-octane and described in Curran et al. [6]. Kinetic modeling predictions are compared to the measured shock tube ignition delay times with good agreement. The new iso-cetane mechanism when combined with previous mechanisms developed by the Lawrence Livermore group for iso-octane [6] and C_7-C_{16} n-alkanes [19-20] comprise an important database for the kinetic simulation of alkanes found in and representative of those found in liquid transportation fuels. Also, the iso-cetane mechanism together with a previously developed n-cetane mechanism allows, for the first time, the simulation of primary reference fuels for diesel with a detailed chemical kinetic model. On the experimental side, the combination of the current iso-cetane ignition time measurements with recent and previous elevated pressure ignition measurements made by the Rensselaer group and others for iso-octane [7-13] and larger n-alkanes (C_7-C_{14}) [10,21-32] comprise a set of kinetic targets for mechanism validation

at engine conditions for cetane and octane rating reference compounds and other alkanes relevant to diesel, gasoline, and jet fuels.

2. Experimental Method and Results

Ignition delay times were measured in the previously described [33] externally-heated high-pressure shock tube at Rensselaer Polytechnic Institute. The shock tube and mixing manifold and vessel, used for preparation, mixing, and storage of reactant mixtures, can be externally heated with electrical resistance silicone heaters. For the iso-cetane experiments described here, the shock tube was heated to temperatures between 100 and 110 ºC. The axial temperature uniformity was routinely monitored, with measured non-uniformity smaller than the ±2.2 ºC uncertainty in the type-K thermocouple measurements; see Fig. 1 for an example axial temperature profile. The thermal uniformity and temperature capability (180 ºC maximum) of the shock tube is enabled by several features of the facility including: a uniform shock tube wall thickness (uniform thermal mass), uniform applied heat flux (same heaters throughout and no gap in heating), uniform and high resistance insulation, and the use of electronic feedback control for controlling current to six heater zones.

Iso-cetane/air mixtures were prepared using 98+% purity degassed liquid 2,2,4,4,6,8,8-heptamethylnonane (iso-cetane) and synthetic air, comprised of 99.995% purity O_2 and N_2 at a molar ratio of 1:3.76. Iso-cetane was introduced into the evacuated mixing vessel via vaporization at the elevated temperature (100-110 ºC) of the mixing vessel and attached manifold and O_2 and N_2 were introduced separately from high-pressure gas cylinders. Mixtures were mixed by a magnetically powered vane assembly

located in the mixing vessel for anywhere from 20 minutes to 2 hours prior to shock tube experiments. Ignition time measurements made at similar conditions (mixture and reflected shock pressure and temperature) show no dependence on mixing time, indicating that mixtures were not influenced by decomposition, oxidation, or wall reactions in the heated mixing vessel. Ignition measurements have previously been made for common mixtures with the shock tube and mixing vessel both heated and unheated showing no discernible influence of heating on the measurements.

Ignition times were determined in the reflected shock region at the driven section end wall location using optical measurement of electronically excited OH (OH*) emission viewed through the shock tube end wall. Piezoelectric pressure measurements were made at five locations spread over the last meter of the driven section for determination of incident shock velocity, needed for calculation of the incident and reflected shock conditions. Additionally, the pressure transducer closest to the end wall (2 cm away) allowed for determination of the time of shock arrival at the end wall as well as providing a second method for ignition time measurements. See Fig. 2 for an example ignition time measurement. For the purposes of defining the ignition delay time, time zero, the time of shock arrival and reflection at the end wall, is determined using measurement of the incident shock passage at a location 2 cm from the end wall and the measured incident shock velocity at the end wall. The time of the onset of ignition at the end wall is defined by extrapolating the maximum slope in OH* emission, viewed through the end wall, to the baseline pre-ignition value.

The reflected shock conditions were determined using the normal shock relations, the known initial conditions (temperature, pressure, and mixture composition), and the

measured incident shock velocity at the end wall. The incident shock velocity at the end wall was determined from the extrapolation of four shock velocity measurements made over the last meter of the driven section with the five pressure transducers. We estimate the uncertainty in initial reflected shock temperature and pressure at ±1.5% and ±2.0% (90% confidence interval), respectively. These uncertainties are primarily due to uncertainty in incident shock velocity and initial temperature, with negligible contribution from uncertainty in initial pressure and mixture composition.

Additionally, this facility, like all shock tubes, displays a non-ideal gasdynamic increase in measured pressure, from the initial reflected shock value, due to boundary layer shock attenuation [31,34-36]. We have previously measured the temporal gradient in pressure in the facility used here to be approximately dP/dt = 2%/ms for test times shorter than 4 ms [13]. Assuming an isentropic relation between pressure and temperature, this results in a change in temperature of dT/dt = ~0.5%/ms. We estimate that this non-ideal gasdynamic behavior shortens the longest measured ignition times reported here (~1 ms) by, at most, 5%. For shorter ignition times, the influence is less.

Ignition delay times were measured for iso-cetane/air mixtures with equivalence ratios of 0.5 and 1.0 for temperatures ranging from 953 to 1347 K and pressures ranging from 8 to 47 atm. For the conditions studied, ignition times varied from 49 to 1160 μs. Measurements were limited to this range by increased uncertainties in shorter ignition times due to uncertainties in determining time-zero and the onset of ignition from the measured pressure and OH* emission traces and by limitations in reflected shock test time for low-temperature (long ignition time) helium-driven shock wave experiments. A tabulation of the experimental data is given in Table 1 and the data are displayed on

Arrhenius axes in Fig. 3. We estimate the uncertainty in measured ignition time at ±25% (90% confidence interval) based on contributions from uncertainties in reflected shock temperature and pressure, reactant mixture composition, and determining the ignition time from the measured OH* emission and pressure. Also, we choose to absorb the non-ideal gasdynamic influence on measured ignition time (~5% reduction in ignition time for the longest ignition time) into the above reported uncertainty.

In Fig. 3 it is can be observed that the data, when plotted on Arrhenius axes, show small scatter about linear least-squares fits. As expected, there is no observed curvature, or negative-temperature-coefficient (NTC) behavior, at the moderate- to high-temperature conditions studied. The ignition time data can be correlated assuming exponential dependence on inverse temperature and power law dependence on pressure and equivalence ratio, as has been shown for other fuels outside of the NTC regime [37], resulting in:

$$\tau = 1.16 \times 10^{-2} P^{-0.72} \Phi^{-0.71} \exp(13200 / T) \ \mu s,$$

where the pressure, P, is in atmospheres and the temperature, T, in Kelvin. In Fig. 4 the ignition times are scaled to a common condition (10 atm, Φ = 1.0), illustrating the adequacy of the correlation (r^2 = 98.9%). Additionally, the data in Fig. 3 is scaled to common pressures (10 and 40 atm) using the power-law pressure dependence obtained in the regression analysis to account for the deviations in reflected shock pressure which result primarily from inconsistent diaphragm rupture, which is exacerbated when the shock tube is heated. The above correlation should not be extrapolated far from the range of conditions studied because different ignition time dependencies will result at different conditions due to inherent differences in the governing chemistry with variation in

pressure, temperature, and O_2 and fuel concentrations (e.g., T-P-[O_2] dependence in the high-temperature regime versus the NTC regime).

3. Kinetic Modeling

The kinetic reaction mechanism for iso-cetane was built in the same modular fashion as in previous studies of large straight-chain and branched alkane fuels [6,15,19,20], using the same 25 reaction types and associated rate expressions as first introduced by Curran et al. [19]. The reaction rate rules were updated for iso-octane [6], and further reaction pathways and reaction rate rules have been proposed [20], but the present mechanism for iso-cetane is nearly identical to those already tested extensively for other fuel molecules.

Reaction pathways for both the high-temperature and low-temperature regimes were included. For the present applications, none of the low-temperature, alkylperoxy radical isomerization pathways was found to be important, even at the highest pressures and lowest temperatures examined in the shock tube experiments. However, inclusion of the low temperature submechanism made it possible to demonstrate that these simulations did not require the alkylperoxy radical isomerization reaction pathways. Also inclusion of the low temperature submechanism allowed extension of the predictions to lower temperatures which are relevant to ignition in a diesel engine. Reaction mechanisms using the same reaction classes and rate rules have been very successful in reproducing shock tube ignition delay times over wide ranges of conditions for large n-alkanes [19,20] and branched alkanes [6,14].

There are considerable structural similarities between iso-octane and iso-cetane, both of which are shown in Fig. 7. Both show the quaternary carbon structure of a carbon atom bonded to 4 other carbon atoms, connected to a secondary carbon atom and then a tertiary carbon atom. The iso-cetane molecule in fact consists of two iso-octyl radicals connected together, and contains 3 of these quaternary carbon atoms. We exploited these very close structural similarities in assembling the detailed kinetic mechanism for iso-cetane, particularly for all of the H atom abstraction reactions. In addition, many of the 8 possible alkyl radicals produced from iso-cetane produce iso-octyl radicals or iso-octene olefin species when they decompose, again leading to many similarities in the reaction mechanisms of the two fuels. The iso-octane mechanism from Curran et al. [6] is actually a significant subset of the iso-cetane mechanism, and we expected before any validation studies that ignition delay times for iso-cetane would be similar to those for iso-octane. In addition, the considerable body of mechanism validation that exists for the iso-octane mechanism provides approximate and indirect validation for the iso-cetane mechanism.

The entire mechanism, with kinetic parameters and required thermochemical data for each species, and including the high and low temperature submechanisms, are available as supplemental material and can also be obtained from the LLNL kinetics web page at http://www-pls.llnl.gov/?url=science_and_technology-chemistry-combustion.

4. Discussion

Kinetic simulations were performed using the present iso-cetane oxidation mechanism, using the Chemkin numerical model with a constant volume, adiabatic approximation, to model the reflected shock region, and the computed results are

compared with the current shock tube ignition delay time measurements in Fig. 5. The maximum deviation between experiment and simulation is a factor of two in ignition time. However, much of the data agrees with the kinetic simulations within the experimental uncertainties, ±25% in ignition time. We consider this agreement to be very good considering the size and complexity of the kinetic mechanism and because the mechanism was developed *a priori* using rate coefficient rules previously developed for aliphatic compounds with no adjustments made to rate parameters for better agreement with the present measurements. The agreement between experiment and mechanism for such a large alkane illustrates that the rate coefficient rules developed for alkanes [6,19-20] can be extended with some confidence at high to moderate temperatures to other fuels where data and mechanisms currently do not exist.

The kinetic model was also used to extend the simulations to temperatures considerably lower than those of the present experiments, and a low temperature reaction regime, including negative temperature coefficient behavior can be seen in Fig. 5, beginning at temperatures below about 900 K. Evidently, ignition data is needed at lower temperatures for more comprehensive mechanism validation, which could be obtained using rapid compression machines or tailored driver gas shock tube methods. Additionally, speciation information obtained using jet-stirred reactors, flow reactors, shock tubes, or other devices would be useful for further probing the oxidation mechanisms for iso-cetane.

While there are no previous iso-cetane ignition data for comparison to the current measurements, the current data can be compared to previous ignition measurements for iso-octane [13] made in the same facility using the same techniques. A comparison of

selected results (40 atm, Φ = 1.0 in air) for iso-cetane and iso-octane is shown in Fig. 6 along with kinetic simulation for the two branched alkanes based on the mechanism presented here for iso-cetane and the iso-octane Curran et al. [6] mechanism. As illustrated in Fig. 6, both the experiments and simulations show that the ignition delay times for iso-octane are somewhat (i.e., 50-100%) longer than those for iso-cetane in the temperature range of the measurements (950-1250 K for conditions displayed). At lower temperatures in the NTC regime the computationally predicted difference is larger, with iso-octane ignition times up to a factor of three longer than those for iso-cetane.

At the moderate temperatures for which experimental data are displayed in Fig. 6, the difference in reactivity between iso-cetane and iso-octane can be attributed to two major factors that are related to the structure of the iso-cetane molecule, shown in Fig. 7. First, 15 of the 18 H bonds in iso-octane are bonded at primary sites in the molecule, while a smaller fraction, 27 out of 34, of the H atoms in iso-cetane are bonded at primary sites. A correspondingly larger fraction of the H atoms in iso-cetane are bonded at secondary and tertiary sites. Since primary C-H bonds are stronger than secondary or tertiary bonds, it is easier and faster to abstract H atoms from iso-cetane. Second, after abstraction of an H atom from either fuel produces a $C_{16}H_{33}$ radical from iso-cetane or a C_8H_{17} radical from iso-octane, iso-cetane produces a greater fraction of reactive H-atoms during the subsequent fragmentation of its alkyl radicals than does iso-octane. H-atoms generated from alkyl radical decomposition provide chain branching through reaction with O_2 ($H + O_2 \rightarrow OH + O$), generating additional radicals which can consume more fuel and intermediates. In contrast, CH_3 radicals generated by alkyl radical decomposition recombine ($CH_3 + CH_3 \rightarrow C_2H_6$), a chain termination step which leads to a smaller and

less reactive intermediate radical pool. The production of H atoms is proportionally greater and the production of methyl radicals is proportionally smaller in iso-cetane than in iso-octane, producing a more rapid ignition of iso-cetane in the temperature range of these experiments. It is important to realize that these distinctions are quite small, producing differences in ignition delay of not more than a factor of two over the range of temperatures studied in the present experiments.

Although outside the range of conditions examined here, it is interesting to note from the computed results in Fig. 6 that at lower temperatures, below 900K, another reaction pathway increases the differences between the iso-cetane and iso-octane ignition times. The increased differences are due to the rates of alkylperoxy radical isomerization ($RO_2 \leftrightarrow QOOH$), which control radical production in the low-temperature oxidation sequence ($R + O_2 \leftrightarrow RO_2 \leftrightarrow QOOH\ (+O_2) \leftrightarrow OOQOOH \rightarrow 2OH$ + products). These reaction pathways are seriously inhibited in the case of iso-octane [6], but for iso-cetane, which has three CH_2 groups appropriately spaced for six-membered transition states for RO_2 isomerization between CH_2 groups [19], these reaction pathways more readily produce radicals than in the case of iso-octane, which has only one CH_2 group. These differences between the mechanisms of iso-cetane and iso-octane ignition at low temperatures are distinct from those differences at higher temperatures that lead to the differences observed in the present experimental results. A more thorough discussion of the low-temperature submechanism for iso-cetane will be the subject of a future publication.

5. Summary

The autoignition of iso-cetane (2,2,4,4,6,8,8-heptamethylnonane), an important cetane number rating reference compound, has been studied at elevated-pressure moderate-temperature conditions (8-47 atm, 953-1347 K, and Φ = 0.5 and 1.0) via measurements of ignition delay in a heated shock tube. Additionally, a new detailed kinetic mechanism has been developed for iso-cetane using reaction rate rules previously employed in mechanisms for iso-octane [6] and large n-alkanes [19-20]. The agreement between mechanism predictions and measured ignition delay times is very good, particularly in light of the large size and complexity of the mechanism and because there has been no adjustment to rate parameters for improved agreement with experiment. The agreement for such a large alkane suggest that the rate coefficient rules developed for aliphatics can be extended to other compounds with confidence at high to moderate temperatures. To our knowledge, the measurements presented here are the first ignition time measurements for iso-cetane and the mechanism presented here is the first detailed iso-cetane mechanism. The data and mechanism contribute toward the kinetic understanding of large alkanes compounds found in transportation fuels and will be useful for developing surrogate mixtures for diesel, jet fuels, and other fuels containing large alkanes. Additionally, the reaction mechanism presented here completes a set of reaction mechanisms for cetane and octane rating reference fuels (n-heptane [19], n-hexadecane [20], iso-octane [6], and iso-cetane).

While there is agreement demonstrated here between experiment and kinetic simulation for the case of the high- to moderate-temperature ignition of iso-cetane, there is still significant opportunity for additional experimental and kinetic modeling work

related to large branched alkanes. For instance, much of the previous work has focused on the highly branched iso-octane (three substituted methyl groups) and here the highly branched iso-cetane (seven substituted methyl groups). However, many branched alkanes found in commercial fuels, particularly Fischer-Tropsch fuels, contain alkanes with only one or two methyl substitutions. Hence, experimental and modeling studies should be extended to less highly branched large alkanes. Additionally, ignition time data is needed at lower temperatures and speciation data is needed at all conditions (low to high temperature and atmospheric to high pressure).

Acknowledgments

The Rensselaer group was supported by the U.S. Air Force Office of Scientific Research (Grant No. FA9550-07-1-0114) with Dr. Julian Tishkoff as technical monitor. MAO and JS are grateful to Michael Tung and Matthew Wilcox for assistance with the shock tube measurements. The computational work in this paper was performed under the auspices of the US Department of Energy, Office of Vehicle Technologies, by the Lawrence Livermore National Laboratory under contract DE-AC52-07NA27344, with Gurpreet Singh and Kevin Stork as program managers.

References

[1] J.T. Farrell, N.P. Cernansky, F.L. Dryer, D.G. Friend, C.A. Hergart, C.K. Law, R. McDavid, C.J. Mueller, H. Pitsch, H. SAE Paper 2007-01-0201, 2007.

[2] Northrop Grumman, Northrop Grumman Petroleum Product Survey Reports, updated annually, http://pps.ms.northropgrumman.com/.

[3] M. Colket, J.T. Edwards, S. Williams, N.P. Cernansky, D.L. Miller, F.N. Egolfopoulos, P. Lindstedt, K. Seshadri, F.L. Dryer, C.K. Law, D.G. Friend, D.B. Lenhert, H. Pitsch, A. Sarofim, M. Smooke, W. Tsang, AIAA Paper AIAA-2007-0770, 2007.

[4] A. Agosta, N.P. Cernansky, D.L. Miller, T. Faravelli, E. Ranzi, Exp. Therm. Fluid Sci. 28 (2004) 701-708.

[5] T. Edwards, L.Q. Maurice, J. Prop. Power 17 (2001**)** 461-466.

[6] H.J. Curran, P. Gaffuri, W.J. Pitz, C.K. Westbrook, Combust. Flame 129 (2002) 253-280.

[7] J.F. Griffiths, P.A. Halford-Maw, D.J. Rose, Combust. Flame 95 (1993) 291-306.

[8] R. Minetti, M. Carlier, M. Ribaucour, E. Therssen, L.R. Sochet, Proc. Combust. Inst. 26 (1996) 747-753.

[9] K. Fieweger, R. Blumenthal, G. Adomeit, Combust. Flame 109 (1997) 599-619.

[10] S. Tanaka, F. Ayala, J.C. Keck, J.B. Heywood, Combust. Flame 132 (2003) 219-239.

[11] D.F. Davidson, B.M. Gauthier, R.K. Hanson, Proc. Combust. Inst. 30 (2005) 1175-1182.

[12] X. He, M.T. Donovan, B.T. Zigler, T.R. Palmer, S.M. Walton, M.S. Wooldridge, A. Atreya, Combust. Flame 142 (2005) 266-275.

[13] H.-P. S. Shen, J. Vanderover, M.A. Oehlschlaeger, Combust. Flame 155 (2008) 739-755.

[14] C.K. Westbrook, W.J. Pitz, H.J. Curran, J. Boercker, W. Kunrath, Int. J. Chem. Kinet. 33 (2001) 868-877.

[15] C.K. Westbrook, W.J. Pitz, J.E. Boercker, H.J. Curran, J.F. Griffiths, C. Mohamed, M. Ribaucour, Proc. Combust. Inst. 29 (2002) 1311-1318.

[16] E.J. Silke, H.J. Curran, J.M. Simmie, Proc. Combust. Inst. 30 (2005) 2639-2647.

[17] J.M. Smith, J.M. Simmie, H.J. Curran, Int. J. Chem. Kinet. 37 (2005) 728-736.

[18] D.B. Lenhert, N.P. Cernansky, D.L. Miller, in: Proc. of the 4th Joint Meeting of the US Sections of the Combustion Institute, 2005.

[19] H.J. Curran, P. Gaffuri, W.J. Pitz, C.K. Westbrook, Combust. Flame 114 (1998) 149-177.

[20] C.K. Westbrook, W.J. Pitz, O. Herbinet, H.J. Curran, E.J. Silke, Combust. Flame 156 (2009) 181-199.

[21] H.K. Ciezki, G. Adomeit, Combust. Flame 93 (1993) 421-433.

[22] R. Minetti, M. Carlier, M. Ribaucour, E. Therssen, L.R. Sochet, Combust. Flame 102 (1995) 298-309.

[23] U. Pfahl, K. Fieweger, G. Adomeit, Proc. Combust. Inst. 26 (1996) 781-789.

[24] J.F. Griffiths, P. Halford-Maw, C. Mohamed, Combust. Flame 111 (1997) 327-337.

[25] B.M. Gauthier, D.F. Davidson, R.K. Hanson, Combust. Flame 139 (2004) 300-311.

[26] J. Herzler, L. Jerig, P. Roth, Proc. Combust. Inst. 30 (2005) 1147-1153.

[27] E. Olchanski, A. Burcat, Int. J. Chem. Kinet. 38 (2006) 703-713.

[28] K. Kumar, Ph.D. Thesis, Case Western Reserve University, 2007.

[29] V.P. Zukhov, V.A. Sechenov, A. Yu. Starikovski, Combust. Flame 153 (2008) 130-136.

[30] D.F. Davidson, D.R. Haylett, R.K. Hanson, Combust. Flame 155 (2008) 108-117.

[31] S.S. Vasu, D.F. Davidson, Z. Hong, V. Vasudevan, R.K. Hanson, Proc. Combust. Inst. 32 (2009), 173-180.

[32] H.-P. S. Shen, J. Steinberg, J. Vanderover, M.A. Oehlschlaeger, Energy Fuels, to appear.

[33] H.-P. S. Shen, M.A. Oehlschlaeger, Combust. Flame, to appear.

[34] E.L. Petersen, R.K. Hanson, Shock Waves 10 (2001) 405-420.

[35] H. Li, Z.C. Owens, D.F. Davidson, R.K. Hanson, Int. J. Chem. Kinet. 40 (2008) 89-98.

[36] M. Chaos, F.L. Dryer, Int. J. Chem. Kinet, to appear.

[37] D.F. Davidson, R.K. Hanson, Int. J. Chem. Kinet. 36 (2004) 510-523.

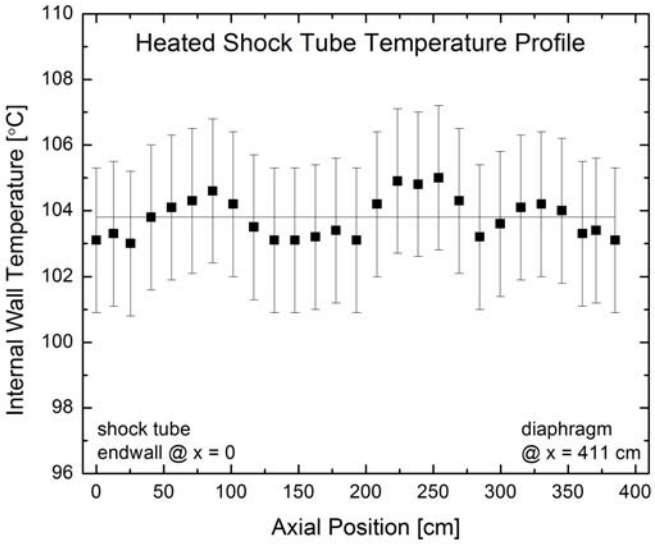

Fig. 1. Typical heated shock tube inner wall temperature profile (driven section).

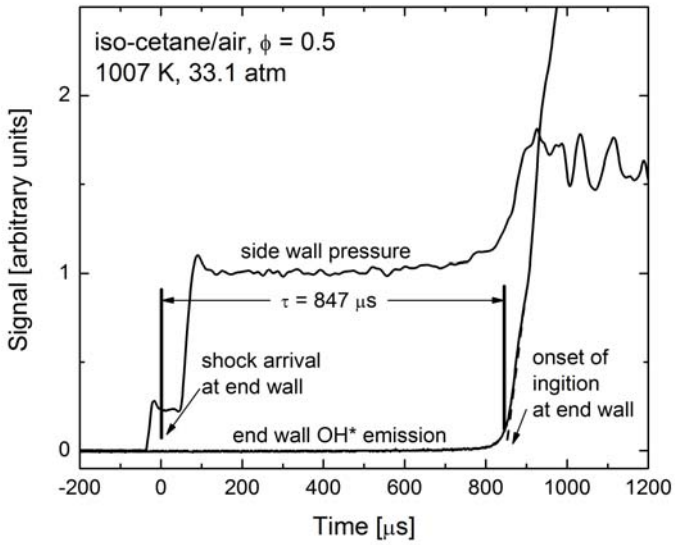

Fig. 2. Example ignition time measurement for a Φ = 0.5 iso-cetane/air mixture.

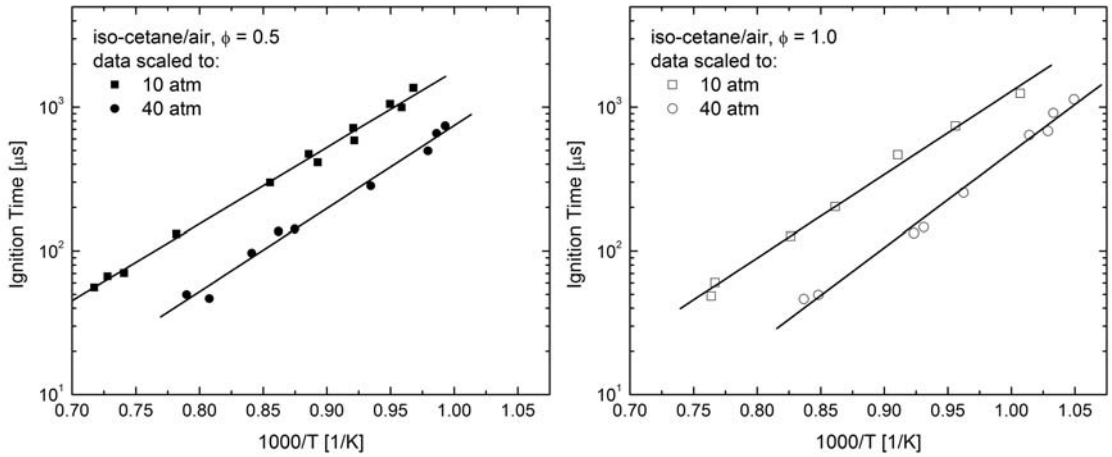

Fig. 3. Ignition time measurements for Φ = 0.5 (left) and Φ = 1.0 (right) iso-cetane/air mixtures. Data scaled to 10 and 40 atm using pressure scaling from regression analysis, $\tau \propto P^{-0.72}$.

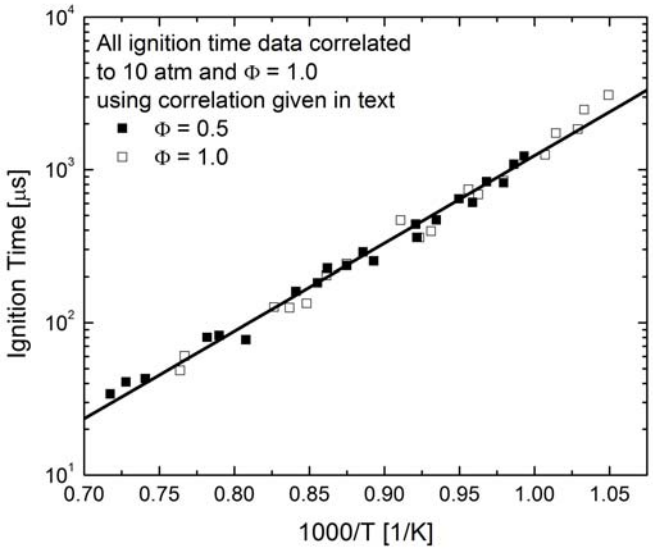

Fig. 4. All ignition time data correlated to a common condition (10 atm and Φ = 1.0) using correlation given in text.

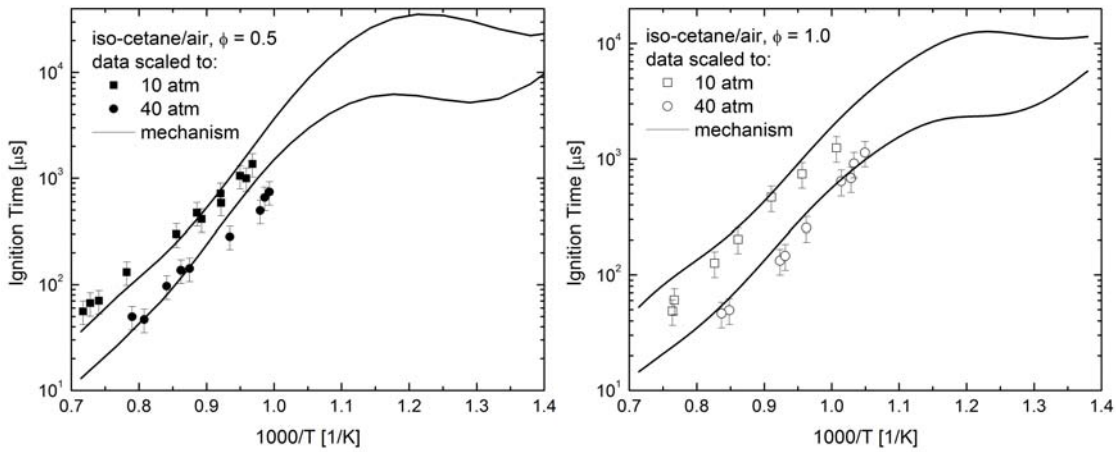

Fig. 5. Measured iso-cetane/air ignition delay times compared to predictions of detailed mechanism.

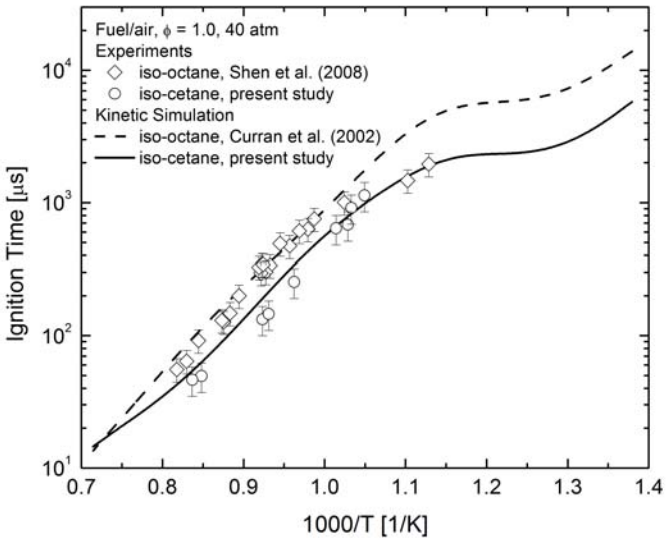

Fig. 6. Measured iso-octane (Shen et al. [13]) and iso-cetane (current study) ignition delay times Φ = 1.0 fuel/air mixtures at 40 atm compared to kinetic predictions based on Curran et al. [6] iso-octane mechanism and current iso-cetane mechanism.

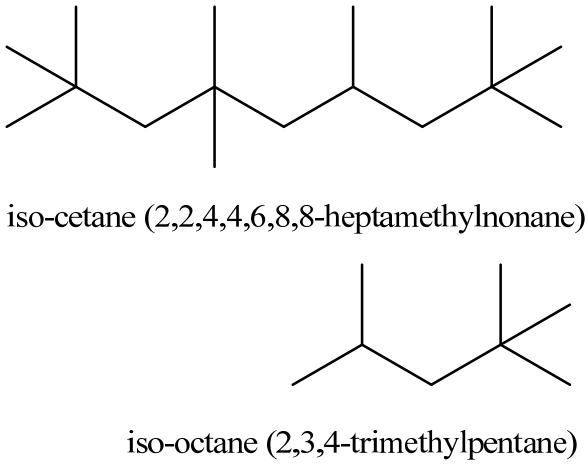

iso-cetane (2,2,4,4,6,8,8-heptamethylnonane)

iso-octane (2,3,4-trimethylpentane)

Fig. 7. Molecular structure of iso-cetane and iso-octane.

Table 1. Measured ignition times for iso-cetane/air mixtures.

iso-cetane/air, Φ = 0.5: 0.4269% iso-cetane, 20.92% O_2, 78.65% N_2			iso-cetane/air, Φ = 1.0: 0.8502% iso-cetane, 20.83% O_2, 78.32% N_2		
P [atm]	T [K]	τ [μs]	P [atm]	T [K]	τ [μs]
14.1	1033	1064	14.0	993	984
8.1	1043	1160	11.7	1046	662
13.4	1053	853	9.8	1098	472
10.9	1085	550	12.5	1161	173
12.5	1086	610	10.9	1210	119
11.5	1120	372	10.4	1304	59
11.8	1129	418	9.9	1309	49
9.0	1169	323	46.9	953	1014
10.4	1279	127	37.1	968	963
10.3	1350	69	31.2	972	813
9.2	1374	71	43.8	986	600
10.7	1394	53	31.8	1039	299
33.1	1007	847	27.0	1074	193
25.9	1014	895	25.4	1083	183
33.1	1021	567	28.5	1179	63
26.9	1070	375	26.5	1195	62
40.7	1143	140			
37.9	1160	142			
40.4	1189	96			
35.3	1238	51			
40.8	1266	49			

Supplementary Material. See enclosed mechanism (Chemkin format) and thermodynamic data (NASA polynomials for use in Chemkin).